SUPPLEMENTAL MATERIAL

The FHI-AIMS code [1] was employed for the DFT calculations. The repeated–slab method was used to model all the systems with the size of the vacuum gap chosen between 16 and 25 Å. In all calculations, a convergence criteria of 10^{-5} electrons for the electron density and 10^{-6} eV for the total energy of the system were used. A convergence criterion of 0.01 eVÅ^{-1} for the maximum final force was used for all structure relaxations. The scaled zeroth-order regular approximation (ZORA) was applied for including relativistic effects.

PTCDA/Me(111)

For Ag(111), a surface unit cell containing two inequivalent PTCDA molecules and 33 atoms per metallic layer was adopted with the adsorption site chosen in agreement with previous investigations [2–5]. For the Au(111) surface, the molecule does not form commensurate monolayers with the surface but rather exhibits a point–on–line growth on the $(22 \times \sqrt{3})$ reconstructed surface [6–9]. The actual situation is not accessible to any type of state-of-the-art modeling. Therefore, as a reasonable approximation, we adopt the same unit cell as used in the Ag case as the differences in the lattice constant between Au and Ag are quite small (4.18 Å and 4.16 Å). For PTCDA/Cu(111), a larger unit cell due to the smaller lattice constant (3.64 Å) is required. We used three models derived by Lorenz Romaner [10], which are based on experimental data [11]. The three initial structures have two inequivalent PTCDA molecules per unit cell. The first one has 44 metal atoms per layer, as the second and third ones are conformed with 50 atoms per metallic layer. The lattice constant was set to the value of 3.64 Å. The main differences among them come from the relative orientation of the PTCDA molecules. We report the most stable one after relaxation.

We used a Monkhorst-Pack [12] grid of $2 \times 2 \times 1$ k–points in the reciprocal space. We used three metallic layers to perform the calculations in-line with previous investigations [4, 10, 13–15]. As in a previous investigation [10], the lattice constants for the PTCDA/Me(111) systems were the PW91 [16] optimized values.

For the calculation of the binding curves, the unrelaxed surface and a planar PTCDA molecule were employed for all the calculated points. The vertical distance d was defined as

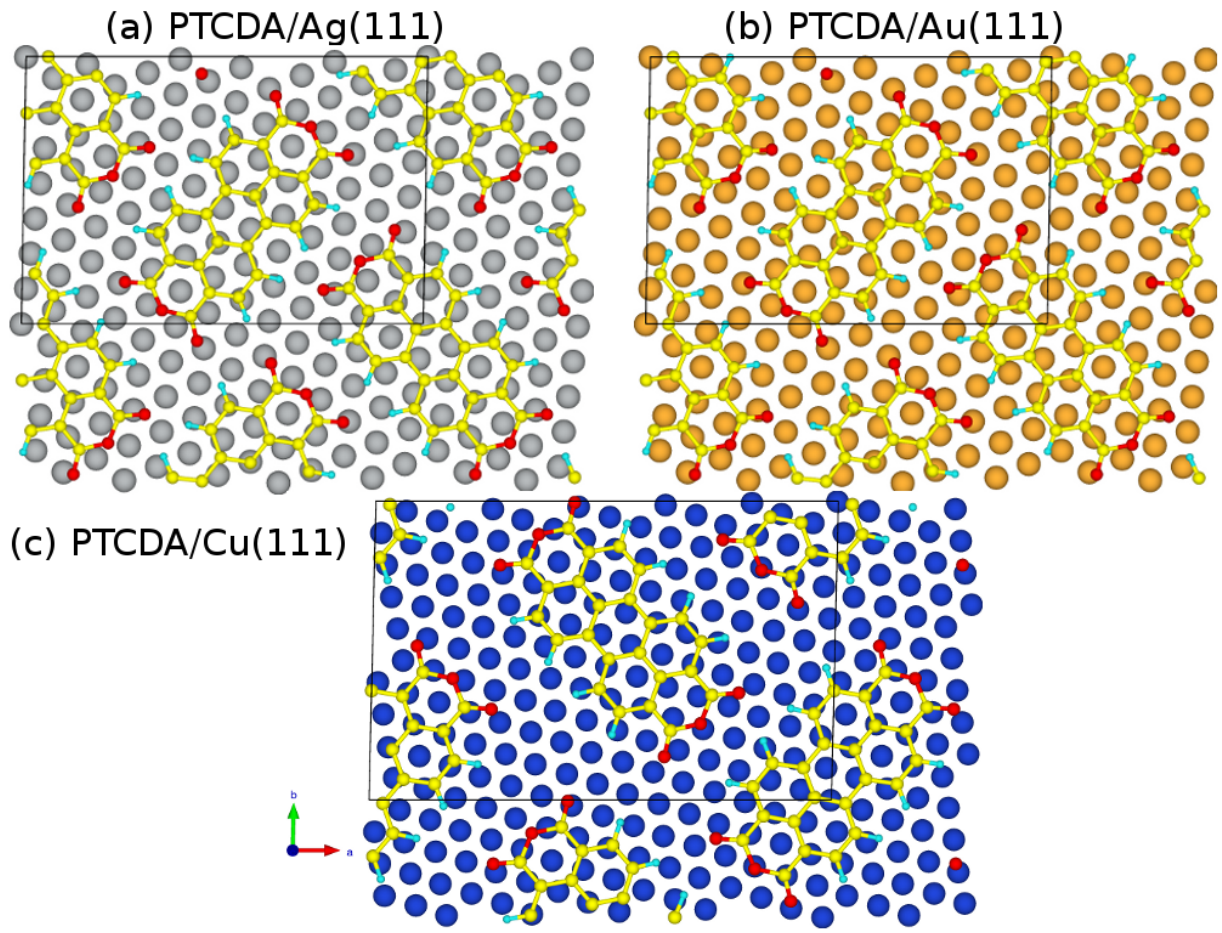

FIG. 1. The structures after relaxation for (a) PTCDA/Ag(111) (b) PTCDA/Au(111), and (c) PTCDA/Cu(111) are presented.

the difference of the position of the molecule with respect to the position of the unrelaxed topmost metallic layer. The adsorption energy per adsorbed molecule was calculated using $E_{ads} = \frac{1}{2}\left[E_{PTCDA/Me} - (E_{Me} + E_{PTCDA})\right]$, where $E_{PTCDA/Me}$ is the energy per unit cell of the PTCDA/Me system, E_{Me} is the energy per unit cell of the isolated metallic slab and E_{PTCDA} is the energy of the isolated PTCDA monolayer with 2 molecules per unit cell.

A structural relaxation was carried out for each of the PTCDA/Me(111) systems. As starting point, the molecule was located at the minimum obtained from the binding curves. The atoms in the PTCDA molecules and the topmost metallic layer were allowed to relax. Figure 1 of this document shows the structure of the PTCDA/Me(111) systems after relaxation. Considering vdW interactions between metal atoms at this point would result in artificial relaxations of the topmost layers of the surface as we use PW91 lattice constants.

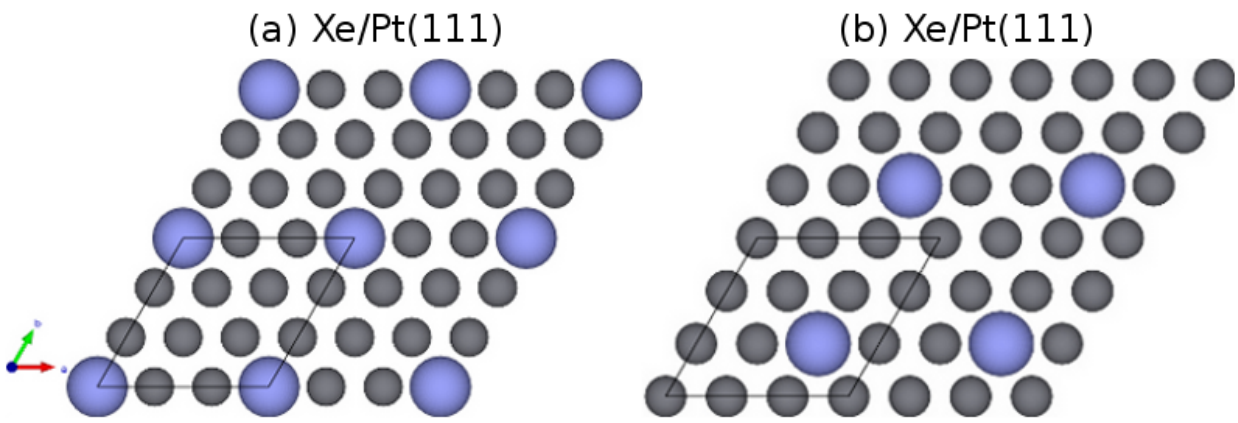

FIG. 2. Structure for the Xe/Pt(111) system with Xe on the (a) top and (b) fcc–hollow adsorption sites after relaxation.

Hence, the vdW interactions between metal atoms were not considered when performing the relaxations. A relaxation of the PTCDA/Ag(111) system using the PBE+vdW$^{\rm surf}$ optimized lattice constant (4.03 Å) and including vdW interactions when performing the relaxation yields a distance for the C–backbone with respect to the unrelaxed topmost layer of 2.91 Å. This represents a difference of $\approx$ 0.07 Å with respect to the number obtained using the PW91 lattice constant value as it is done in this work.

Xe/Me(111)

For the Xe/Me(111) systems, the experimentally reported $(\sqrt{3}\times\sqrt{3})$R30° structure with top and fcc–hollow adsorption sites were adopted for all different metals. The Pt/Xe(111) system with Xe on the top and fcc–hollow adsorption sites is shown in Fig. 2.

We used a Monkhorst-Pack grid of $15 \times 15 \times 1$ k–points in the reciprocal space and six metallic layers to perform the calculations. The PBE [17] optimized lattice constant was used to create all the metallic slabs: 4.15, 3.63, 3.97, and 3.94 Å for Ag, Cu, Pt, and Pd, respectively.

A structural relaxation was performed for all the systems where the Xe atom and the atoms in the topmost and first subsurface metallic layers were allowed to relax. As mentioned before, we do not consider vdW interactions between metal atoms in order to avoid an

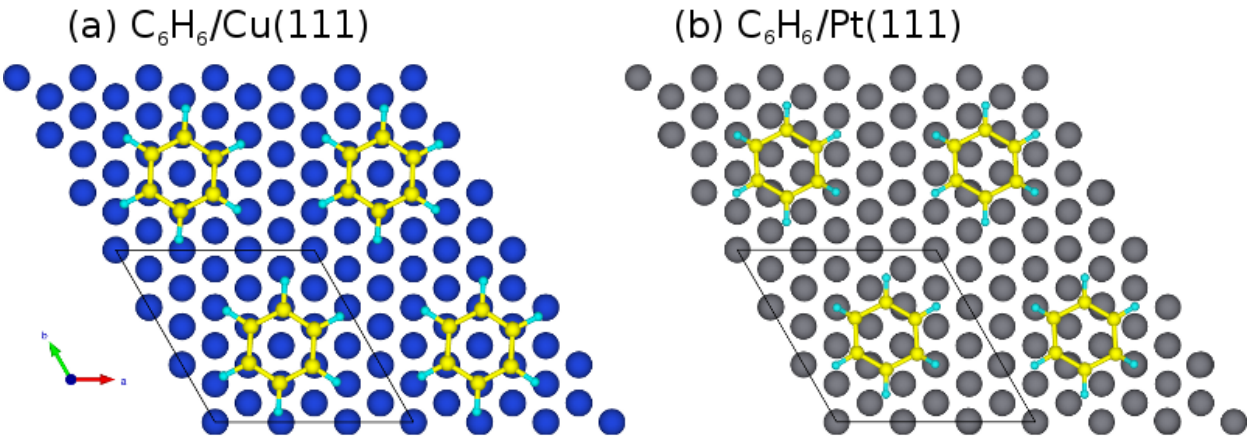

FIG. 3. (a) The hcp 30° site for C_6H_6/Cu(111) and (b) the bridge 30° site for C_6H_6/Pt(111). Both structures are reported after relaxation.

artifical relaxation of the surface.

In all cases, we find that both adsorption sites, top and fcc–hollow, are practically degenerate. For Xe/Pt(111), measurements show that at low coverage, the difussion barrier for lateral movement of the Xe atoms on the surface is less than 10 meV [18]. We report, nonetheless, the Xe-surface distance for the top site because it is experimentally determined as the most stable one [19, 20]. The distances $d_{Ads-Sub}$ in Table II of the main text are reported with respect to the average distance of the topmost metallic layer. Zero-point vibrational energy (ZPVE) in the harmonic approximation was also included in the adsorption energies.

C_6H_6/Me(111)

For C_6H_6/Me(111), we used a (3×3) unit cell as experimental data for these structures is not available. Benzene can adsorb at the high-symmetry site (atop, bridge, fcc, and hcp) of the metal surface. Each site can be either 0° or 30° orientated, denoting the angle of rotation of the C-C bonds with respect to the metal-metal bond in the substrate [21, 22]. For the case of C_6H_6 on Ag(111) and Cu(111), the reported results are for benzene located at the hcp 30° site. In the case of Pt(111) and Pd(111), the reported values are for the bridge 30° site. These structures are considered to be the most stable ones [21, 22]. Figure 3

shows the hcp 30° and the bridge 30° sites for Cu and Pt respectively after relaxation.

We used a Monkhorst-Pack grid of $15 \times 15 \times 1$ k–points in the reciprocal space and six metallic layers to perform the calculations. The lattice constant for these systems was also set to the PBE optimized values.

A structural relaxation was carried out for each of the C_6H_6/Me(111) systems. The atoms in the benzene molecule and in the topmost and first subsurface metallic layers were allowed to relax, vdW interactions between metal atoms were not considered. Zero-point vibrational energy (ZPVE) in the harmonic approximation was also included in the adsorption energies.

The experimental adsorption energies were estimated using temperature-programmed desorption (TPD) data for benzene on Cu(111) and Ag(111), as listed in Table II of the main text. This was achieved by using the Redhead formula [23] for the range of preexponential factors 10^{15}-10^{18} s^{-1} , that is typical for large molecules adsorbed on transition metal surfaces [24–26]. For C_6H_6/Pt(111), the heat of adsorption was measured directly by microcalorimetry. The presumed error of these measurements was estimated to be 10% by the authors [27].

[1] V. Blum *et al.*, Comput. Phys. Commun. **180**, 2175 (2009).

[2] K. Glöckler *et al.*, Surf. Sci. **405**, 1 (1998).

[3] L. Kilian, E. Umbach, and M. Sokolowski, Surf. Sci. **573**, 359 (2004).

[4] M. Rohlfing, R. Temirov, and F. Tautz, Phys. Rev. B **76**, 115421 (2007).

[5] A. Hauschild *et al.*, Phys. Rev. B **81**, 125432 (2010).

[6] P. Fenter *et al.*, Phys. Rev. B **56**, 3046 (1997).

[7] L. Killian, E. Umbach, and M. Sokolowski, Surf. Sci. **600**, 2633 (2006).

[8] S. Mannsfeld *et al.*, Org. Electron. **2**, 121 (2001).

[9] T. T. Schmitz–Hübsch *et al.*, Phys. Rev. B **55**, 7972 (1997).

[10] L. Romaner *et al.*, New J. Phys. **11**, 053010 (2009).

[11] T. Wagner *et al.*, J. Phys.: Condens. Matter **19**, 056009 (2007).

[12] H. Monkhorst and J. Pack, Phys. Rev. B **50**, 17953 (1976).

[13] A. Hauschild *et al.*, Phys. Rev. Lett. **94**, 036106 (2005).

[14] S. Picozzi *et al.*, Phys. Rev. B **68**, 195309 (2003).

[15] M. Rohlfing and T. Bredow, Phys. Rev. Lett. **101**, 266106 (2008).

[16] J. P. Perdew *et al.*, Phys. Rev. B **46**, 6671 (1992).

[17] J. Perdew, K. Burke, and M. Ernzerhof, Phys. Rev. Lett. **77**, 3865 (1996).

[18] J. Ellis, A. P. Graham, and J. P. Toennies, Phys. Rev. Lett. **82**, 5072 (1999).

[19] R. D. Diehl *et al.*, J. Phys.: Condens. Matter **16**, S2839 (2004).

[20] G. Vidali *et al.*, Surf. Sci. Rep. **12**, 133 (1991).

[21] K. Berland, T. Einstein, and P. Hyldgaard, Phys. Rev. B **80**, 155431 (2009).

[22] W. Gao, W. T. Zheng, and Q. Jiang, J. Chem. Phys **129**, 164705 (2008).

[23] P. A. Redhead, Vacuum **12**, 203 (1962).

[24] R. Z. Lei, A. J. Gellman, and B. E. Koel, Surf. Sci. **554**, 125 (2004).

[25] K. A. Fichthorn and R. A. Miron, Phys. Rev. Lett. **89**, 196103 (2002).

[26] S. L. Tait, Z. Dohnalek, C. T. Campbell, and B. D. Kay, J. Chem. Phys. **122**, 164708 (2005).

[27] H. Ihm, H. Ajo, J. Gottfried, P. Bera, and C. Campbell, J. Phys. Chem. B **108**, 14627 (2004).